# Intermediate state representation approach to physical properties of electronically excited molecules

J. Schirmer
*Physikalisch-Chemisches Institut, University of Heidelberg, D-69120 Heidelberg, Germany*

A. B. Trofimov
*Laboratory of Quantum Chemistry, Irkutsk State University, 66403 Irkutsk, Russian Federation*

(Received 2 March 2004; accepted 30 March 2004)

Propagator methods provide a direct approach to energies and transition moments for (generalized) electronic excitations from the ground state, but they do not usually allow one to determine excited state wave functions and properties. Using a specific intermediate state representation (ISR) concept, we here show how this restriction can be overcome in the case of the algebraic–diagrammatic construction (ADC) propagator approach. In the ISR reformulation of the theory the basic ADC secular matrix is written as a representation of the Hamiltonian (or the shifted Hamiltonian) in terms of explicitly constructable states, referred to as intermediate (or ADC) states. Similar intermediate state representations can be derived for operators other than the Hamiltonian. Together with the ADC eigenvectors, the intermediate states give rise to an explicit formulation of the excited wave functions and allow one to calculate physical properties of excited states as well as transition moments for transitions between different excited states. As for the ground-state excitation energies and transition moments, the ADC excited state properties are size consistent so that the theory is suitable for applications to large systems. The established hierarchy of higher-order $[\mathrm{ADC}(n)]$ approximations, corresponding to systematic truncations of the IS configuration space and the perturbation–theoretical expansions of the ISR matrix elements, can readily be extended to the excited state properties. Explicit ISR matrix elements for arbitrary one-particle operators have been derived and coded at the second-order $[\mathrm{ADC}(2)]$ level of theory. As a first computational test of the method we have carried out ADC(2) calculations for singlet and triplet excited state dipole moments in $H_2O$ and HF, where comparison to full CI results can be made. The potential of the ADC(2) method is further demonstrated in an exploratory study of the excitation energies and dipole moments of the low-lying excited states of paranitroaniline. We find that four triplet states, T1–T4, and two singlet states, S1 and S2, lie (vertically) below the prominent charge transfer (CT) excitation, S3. The dipole moment of the S3 state $(17.0D)$ is distinctly larger than that of the corresponding T3 triplet state $(11.7D)$. © *2004 American Institute of Physics.*
[DOI: 10.1063/1.1752875]

## I. INTRODUCTION

For a detailed understanding of the processes following electronic excitation of molecules in the gas phase or in a solvent, it is important to characterize the excited states beyond the pure energetics also with respect to certain key physical properties, e.g., their dipole moments. Such excited state (ES) properties and, more general, transition moments for transitions between different excited states (ES moments) can readily be deduced from the excited state wave function. In practice, however, the computation of ES properties and moments is always a demanding task. To illustrate that point it may be instructive to go briefly through the various ways of how ES properties and moments are treated in the major contemporary quantum chemical methods.

In the standard configuration interaction (CI) treatment, the computation of ES properties and moments is straightforward. However, the applicability of the CI method to larger molecules is restricted due to the inherent size-consistency error (for example, see Helgaker *et al.*[1]), which is expected to be even more pronounced for properties than for excitation energies. It is for these limitations that the CI method has given way to alternative, size-consistent wave function methods, such as the coupled-cluster (CC) methods and the complete active space second-order perturbation theory (CASPT2) approach.[2,3]

The CC methods, comprising three related developments referred to as coupled-cluster linear response (CCLR),[4–6] equation-of-motion coupled cluster (EOM–CC),[7–9] and symmetry-adapted cluster configuration interaction (SAC–CI),[10–12] lead to a twofold wave function representation of the excited states, corresponding to the right and left eigenvectors of the non-Hermitian CC secular matrix. In forming meanigful matrix elements for ES property, one has to use both the right and left ES representations. As was demonstrated by Koch *et al.*[13] in the case of ground state transition moments, the most obvious form of such matrix elements is not size consistent. A size consistent, though much more complicated expression was derived within the CCLR theory by Christiansen *et al.*[14,15] Presently, the proper ES property and moments are available only for a part of the

 

CC approximation hierarchy (CCSD and CC2) and here, moreover, restricted to singlet excitations.

Another widely used wave function method for electronic excitation in molecules is the CASPT2 method established by Roos and collaborators.[2,3] As a specific feature of the CASPT2 method, one uses individually optimized sets of molecular orbitals (MO) for different states. This has the consequence that the evaluation of transition moments for such states can become quite cumbersome. An indication of this and other difficulties may be seen in the instance that in most if not all of the previous CASPT2 studies the results reported for transition moments and excited state properties have been obtained at the lower CASSCF level of theory.

Methods not being based on a wave function (WF) approach have proved to be a viable alternative in the treatment of electronic excitation in molecules. An increasingly popular method of the latter type is the time-dependent density functional theory (TDDFT).[16,17] The TDDFT equations, describing the linear response of the ground-state density to a time-dependent perturbation, allow one to compute directly excitation energies and (ground-to-excited state) transition moments, but do not give access to the excited state wave functions. As far as ES properties are concerned, an obvious way out is to determine these quantities as analytical derivatives of the (excitation) energies with respect to the ''strength'' of an additional (''external'') potential associated with the property operator under consideration. Analytical TDDFT derivatives have been worked out, for example, by Van Caillie and Amos[18,19] and used by Burcl *et al.*[20] to compute ES dipole moments for the furan and pyrrole molecules. As the latter authors find, the dipole moments computed that way are very sensitive to the form of the chosen DFT functional. Apparently, much more testing and comparing with other theoretical results, preferably FCI data, will be needed before one can confidently rate the quality of the TDDFT ES properties.

Other non-WF methods, deriving from the theory of the polarization propagator,[21] such as the second-order polarization propagator approach (SOPPA)[22–24] and the algebraic–diagrammatic construction (ADC) schemes,[25–28] have been used in the computation of molecular electronic excitation spectra for a long time. As is well known, the propagator methods allow for the direct computation of excitation energies and transition moments for transitions from the ground state, but the underlying concept does not aim at determining ES wave functions and properties. The latter is a real constraint for approximation strategies based on the characteristic diagrammatic perturbation theory for the polarization propagator, such as the ADC methods. The SOPPA method, by contrast, being based on the so-called superoperator formalism[29] or the essentially equivalent equation-of-motion (EOM) approach,[30,31] leads to explicit representations of the excited states that can be used to compute ES properties. It seems, though, that attempts to exploit this potential of the superoperator based methods have been rather scarce (see, for example, the computations of Weiner and Öhrn[32] for ES dipole moment curves of the LiH molecule).

As for the ADC approach, the unsatisfactory present status with respect to ES properties and moments can be overcome in both an elegant and practical way, as will be described in this contribution. The development is based on the finding that the ADC secular matrix can be formulated as the representation of the Hamiltonian in terms of a basis set of explicitely constructable intermediate states.[33,34] Together with the ADC eigenvectors, the intermediate states lead to an explicit representation of the excited state wave functions, which can be used to compute arbitrary ES properties and moments provided a reliable and practical approximation for the intermediate state representation (ISR) of the respective property operator is available. In the following we report on the derivation and computer implementation of the ISR for an arbitrary one-particle operator at the level of the second-order ADC approximation. This ISR/ADC(2) method allows for a consistent treatment of ES properties and moments for singly excited states through second order of perturbation theory. For a first numerical test of the method, small model computations were carried out for the HF and $H_2O$ molecules both at the ADC(2) and full(F) CI level of theory. The comparison of the ADC(2) and FCI dipole moments is very encouraging, especially when the ADC(2) dipole moment ISR matrix is used together with the eigenvectors of the ADC(3) secular problem. To explore the potential of the present approach in the case of a realistic system, a large-scale ADC(2) study was conducted for the lowest singlet and triplet excitations in the paranitroaniline (PNA) molecule. PNA is an interesting testing ground for any ES property method, because, as is well known, some of its excited states have strongly polar charge-transfer (CT) character and, thus, large dipole moments.

An outline of the paper is as follows: The ensuing Sec. II gives a brief review of the concept of intermediate state representations in the case of electron excitation. In Sec. III the ISR concept is extended to the representation of an arbitrary one-particle operator, which allows us to determine excited state properties and transition moments at well-defined levels of approximation. Some general aspects of the development, in particular, the truncation error and the size consistency of the ISR formulation, are discussed in Sec. IV. First numerical tests and an exemplary application to PNA are presented in Secs. V and VI, respectively. A brief summary and some conclusions are given in the final Sec. VII.

## II. REVIEW OF INTERMEDIATE STATE REPRESENTATIONS

The concept of intermediate state representations (ISR) has been presented at length elsewhere (see Refs. 27, 34, and 35), so that we may confine us here to a brief review.

In the ISR approach to electronic excitation the exact excited states $|\Psi_n\rangle$ are expanded according to

$$|\Psi_n\rangle = \sum_J X_{Jn} |\tilde{\Psi}_J\rangle \tag{1}$$

in terms of a complete set of intermediate states $|\tilde{\Psi}_J\rangle$. The intermediate states derive from the so-called correlated excited states

$$|\Psi_J^0\rangle = \hat{C}_J |\Psi_0\rangle \tag{2}$$

obtained by applying the "physical" excitation operators $\hat{C}_J$ to the exact ground state $|\Psi_0\rangle$. The manifold

$$\{\hat{C}_J\}=\{c_a^\dagger c_k;\ c_a^\dagger c_b^\dagger c_k c_l, a<b, k<l;\ \ldots\} \tag{3}$$

of the excitation operators comprises particle–hole $(p-h)$, two-particle–two-hole $(2p-2h)$, etc., excitations. Here the second-quantized operators $c_p^\dagger(c_p)$ are associated with one-particle states (spin–orbitals) $|\phi_p\rangle$, usually ground-state Hartree–Fock(HF) orbitals. Following a widely used notation, the subscripts $a,b,c,\ldots$ and $i,j,k,\ldots$ refer to unoccupied (virtual) and occupied orbitals, respectively, while the letters $p,q,r,\ldots$ will be used in the general case.

The intermediate states $|\tilde{\Psi}_J\rangle$ are constructed by applying a specific orthonormalization procedure to the correlated excited states. The essential step here is Gram–Schmidt orthogonalization of the successive $p-h$, $2p-2h,\ldots$ excitation classes $\mu=1,2,\ldots$, including the ground state as a zeroth excitation class. For illustration let us consider the construction of the intermediate $p-h$ states. Orthogonalization with respect to the ground state leads to the "precursor" states

$$|\Psi_{ak}^{\#}\rangle=c_a^\dagger c_k|\Psi_0\rangle-|\Psi_0\rangle\langle\Psi_0|c_a^\dagger c_k|\Psi_0\rangle. \tag{4}$$

In a second step the intermediate states can be formed according to

$$|\tilde{\Psi}_{ak}\rangle=\sum|\Psi_{bl}^{\#}\rangle(S^{-1/2})_{bl,ak} \tag{5}$$

by symmetrical orthonormalization of the precursor states. Here $\mathbf{S}$ is the overlap matrix of the precursor states,

$$S_{ak,bl}=\langle\Psi_0|c_k^\dagger c_a c_b^\dagger c_l|\Psi_0\rangle - \langle\Psi_0|c_k^\dagger c_a|\Psi_0\rangle\langle\Psi_0|c_b^\dagger c_l|\Psi_0\rangle. \tag{6}$$

The intermediate states establish a matrix representation of the Hamiltonian $\hat{H}$ or likewise of the "subtracted" Hamiltonian $\hat{H}-E_0$, where $E_0$ is the (exact) ground state energy,

$$M_{IJ}=\langle\tilde{\Psi}_I|\hat{H}-E_0|\tilde{\Psi}_J\rangle. \tag{7}$$

The Schrödinger equation for the excited states (1) leads to the following Hermitian eigenvalue problem:

$$\mathbf{MX}=\mathbf{X\Omega},\quad \mathbf{X}^\dagger\mathbf{X}=\mathbf{1} \tag{8}$$

for the ISR secular matrix $\mathbf{M}$. Here $\mathbf{\Omega}$ denotes the diagonal matrix of eigenvalues $\Omega_n$, and $\mathbf{X}$ is the matrix of eigenvectors. Obviously, the eigenvalues can be identified as the excitation energies,

$$\Omega_n=E_n-E_0 \tag{9}$$

while the eigenvector components are the expansion coefficients in the IS expansion (1) of the excited states.

For the evaluation of spectral intensities one must consider transition moments of the form

$$T_n=\langle\Psi_n|\hat{D}|\Psi_0\rangle \tag{10}$$

for a pertinent (one-particle) operator

$$\hat{D}=\sum_{r,s} d_{rs}c_r^\dagger c_s. \tag{11}$$

Here

$$d_{rs}=\langle\phi_r|\hat{d}|\phi_s\rangle \tag{12}$$

denote the one-particle matrix elements associated with $\hat{D}$. In the ISR formulation the transition moments can be written as

$$T_n=\sum_J X_{Jn}^* F_J, \tag{13}$$

where

$$F_J=\langle\tilde{\Psi}_J|\hat{D}|\Psi_0\rangle \tag{14}$$

are referred to as ISR transition moments (for the operator $\hat{D}$). The latter quantities can be further expanded according to

$$F_J=\sum_{r,s} f_{J,rs}d_{rs}, \tag{15}$$

where

$$f_{J,rs}=\langle\tilde{\Psi}_J|c_r^\dagger c_s|\Psi_0\rangle \tag{16}$$

are referred to as ISR transition amplitudes.

Approximations based on the ISR formulation can be obtained by truncating the configuration space and using perturbation expansions for the ISR secular matrix elements and transition amplitudes,

$$\mathbf{M}=\mathbf{M}^{(0)}+\mathbf{M}^{(1)}+\mathbf{M}^{(2)}+\cdots, \tag{17}$$

$$\mathbf{f}=\mathbf{f}^{(0)}+\mathbf{f}^{(1)}+\mathbf{f}^{(2)}+\cdots. \tag{18}$$

Here the familiar Møller–Plesset partitioning

$$\hat{H}=\hat{H}_0+\hat{H}_I \tag{19}$$

of the Hamiltonian is supposed. The truncation of the configuration space and the truncation of the perturbation series in the sub-blocks of $\mathbf{M}$ and $\mathbf{f}$ can be done in a systematical and consistent way, leading to a hierarchy of higher-order approximation schemes.

A practical way of deriving such ISR approximations is based on the so-called algebraic–diagrammatic construction (ADC) procedure for the polarization propagator.[21] The essential idea here is to compare the IS representation (or ADC form) of the propagator with its original diagrammatic perturbation series[25,27] through a given order $n$ of perturbation theory. This leads in a natural way to explicit perturbation–theoretical expressions for the matrix elements of $\mathbf{M}$ and $\mathbf{f}$ establishing the $n$th order [ADC($n$)] approximation schemes. While the ADC(2) approximation has been available for a long time,[25] the ADC procedure could recently be extended to the third-order level.[27]

In principle, the perturbation expansions for $\mathbf{M}$ and $\mathbf{f}$ can also be deduced from the closed-form expressions for the sub-blocks of $\mathbf{M}$ and $\mathbf{f}$ deriving from the ISR construction procedure (see Ref. 33). These expressions depend on the exact ground state $|\Psi_0\rangle$ and the ground state energy $E_0$, so that the familiar Rayleigh–Schrödinger perturbation theory can be used to derive the desired expansions (17) and (18). However, the latter procedure becomes quite cumbersome

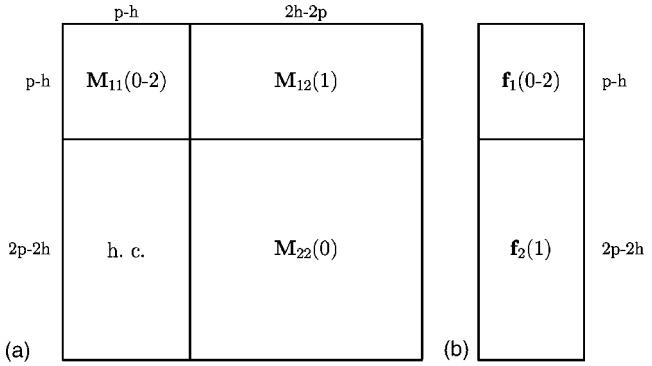


FIG. 1. Block structure of the second-order ADC(2) secular matrix **M** and transition amplitude matrix **f**. The numbers in brackets indicate the orders of terms to be considered in the perturbation expansions of the matrix elements.

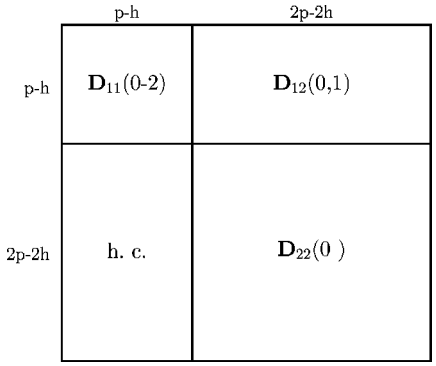


FIG. 2. Block structure of the second-order ISR [or ADC(2)] matrix **D** for a single-particle operator $\hat{D}$. The numbers in brackets indicate the orders of terms to be considered in the perturbation expansions of the matrix elements.

beyond second order and has so far only been used to rederive the ADC(2) equations for the electron propagator.[33]

Figure 1 shows schematically the block structure of the ISR secular matrix **M** and the matrix of transition amplitudes **f** at the ADC(2) and ADC(3) level. In both cases the explicit configuration space is spanned by the $p-h$ and $2p-2h$ excitations. As indicated in Fig. 1, the perturbation expansions of the ADC(2) secular matrix elements extend through second, first, and zeroth order in the $p-h$ diagonal block, $p-h/2p-2h$ coupling block, and $2p-2h$ diagonal block, respectively. At the ADC(3) level, these perturbation expansions are extended to third, second, and first order, respectively.

It should be noted that the ADC–ISR method can also be used to compute absolute energies. For this purpose one needs the IS representation of $\hat{H}$, which according to

$$\tilde{H}_{IJ}=\langle\tilde{\Psi}_I|\hat{H}|\tilde{\Psi}_J\rangle=M_{IJ}+E_0\delta_{IJ} \tag{20}$$

differs from **M** by the constant diagonal matrix $E_0\mathbf{1}$.

## III. PHYSICAL PROPERTIES OF EXCITED STATES AND EXCITED STATE TRANSITION MOMENTS

To characterize an excited state $|\Psi_n\rangle$ with respect to a physical quantity other than the energy, e.g., the dipole moment, one has to evaluate the expectation value

$$D_n=\langle\Psi_n|\hat{D}|\Psi_n\rangle \tag{21}$$

for the corresponding operator $\hat{D}$. Here and in the following we will confine us to the case of a one-particle operator as given by Eq. (11). In the ISR formulation $D_n$ is obtained according to

$$D_n=\underline{X}_n^\dagger\tilde{\mathbf{D}}\underline{X}_n \tag{22}$$

from the $n$th eigenvector $\underline{X}_n$ of the ADC secular problem and the matrix $\tilde{\mathbf{D}}$,

$$\tilde{D}_{IJ}=\langle\tilde{\Psi}_I|\hat{D}|\tilde{\Psi}_J\rangle \tag{23}$$

referred to as IS representation of $\hat{D}$. In a similar way, one may express the transition moments between two (distinct) excited states according to

$$T_{nm}=\langle\Psi_n|\hat{D}|\Psi_m\rangle=\underline{X}_n^\dagger\tilde{\mathbf{D}}\underline{X}_m, \quad n\neq m. \tag{24}$$

It is useful to write $\tilde{\mathbf{D}}$ in the form

$$\tilde{D}_{IJ}=D_0\delta_{IJ}+D_{IJ}, \tag{25}$$

where

$$D_0=\langle\Psi_0|\hat{D}|\Psi_0\rangle \tag{26}$$

is the ground-state expectation value of $\hat{D}$ and **D** is the IS representation of the ''subtracted'' operator $\hat{D}-D_0$. This form of the ISR matrix elements will be retrieved in a natural way in the perturbation–theoretical developments discussed below. It allows one to write the total excited state expectation value, $D_n$, as the sum of a ground state contribution, $D_0$, and a transition contribution, $\Delta D_n=D_n-D_0$. In the expression for the transition moments, Eq. (24), $\tilde{\mathbf{D}}$ can obviously be replaced by **D**.

In analogy to Eq. (18) there is a perturbation expansion

$$\mathbf{D}=\mathbf{D}^{(0)}+\mathbf{D}^{(1)}+\mathbf{D}^{(2)}+\cdots, \tag{27}$$

for the matrix **D**. Our aim is to deduce the explicit perturbation expansions for the matrix elements of **D** required at the second-order [ADC(2)] level of approximation. Together with the ADC(2) eigenvectors this will yield consistent excited state expectation values and transition moments for singly excited states through second order. In contrast to the case of the secular matrix, one cannot make use of the ADC procedure and its diagrammatic techniques here but rather must resort to the more tedious approach via the explicit construction of the intermediate states. Obviously, the following contributions have to be considered in the subblocks of **D** (see Fig. 2):

$$\mathbf{D}_{11}=\mathbf{D}_{11}^{(0)}+\mathbf{D}_{11}^{(1)}+\mathbf{D}_{11}^{(2)},$$

$$\mathbf{D}_{12}=\mathbf{D}_{12}^{(0)}+\mathbf{D}_{12}^{(1)},$$

$$\mathbf{D}_{22}=\mathbf{D}_{22}^{(0)}.$$

Here the subscripts 1,2 label collectively $p-h$ and $2p-2h$ entries, respectively.

The zeroth-order contributions can readily be evaluated, as here the intermediate states are given by the HF configurations,

$$|\Psi_J^{(0)}\rangle = \hat{C}_J|\Phi_0\rangle = |\Phi_J\rangle \tag{28}$$

yielding

$$D_{IJ}^{(0)} = \langle\Phi_I|\hat{D}|\Phi_J\rangle - \delta_{IJ}\langle\Phi_0|\hat{D}|\Phi_0\rangle. \tag{29}$$

Here $|\Phi_0\rangle$ denotes the HF ground state. Inspection of the first-order contributions shows that $\mathbf{D}_{11}^{(1)}=\mathbf{0}$, and it remains to determine the second-order contributions in the $p-h$ diagonal block, $\mathbf{D}_{11}^{(2)}$, and the first-order contributions in the $p-h/2p-2h$ coupling block, $\mathbf{D}_{12}^{(1)}$. Clearly the most demanding task is posed by $\mathbf{D}_{11}^{(2)}$. Here the the intermediate states $|\tilde{\Psi}_{ak}\rangle$ must be expanded through second order. To get an idea of how to proceed let us consider the following result obtained from Eqs. (4), (5), and (6) by omitting third- and higher order contributions:

$$|\tilde{\Psi}_{ak}\rangle = (c_a^\dagger c_k - \rho_{ka}^{(2)})|\Psi_0\rangle - \sum_{a'k'} c_{a'}^\dagger c_{k'}|\Psi_0\rangle\, \tfrac{1}{2}S_{ak,a'k'}^{(2)} + O(3). \tag{30}$$

Here we have used that the precursor overlap matrix $\mathbf{S}$ has a perturbation expansion of the form $\mathbf{S}=\mathbf{1}+\mathbf{S}^{(2)}+O(3)$, so that $\mathbf{S}^{-1/2}=\mathbf{1}-\frac{1}{2}\mathbf{S}^{(2)}+O(3)$; $\boldsymbol{\rho}^{(2)}$ is the second-order one-particle density matrix. Now the explicit Rayleigh–Schrödinger expansion $|\Psi_0\rangle=|\Psi_0^{(0)}\rangle+|\Psi_0^{(1)}\rangle+|\Psi_0^{(2)}\rangle$ can be used on the rhs of Eq. (30), discarding terms beyond second order. The resulting expression may finally be inserted in the desired matrix element $\langle\tilde{\Psi}_{ak}|\hat{D}|\tilde{\Psi}_{a'k'}\rangle$, where again third- and higher order contributions are omitted. A brief sketch of the somewhat lengthy, though straightforward algebra required in these derivations and the final results are given in the Appendix.

Let us briefly comment on the evaluation of the ground-state expectation value $D_0$ entering the diagonal of the ISR matrix according to Eq. (25). As is well known, this quantity may be written as

$$D_0 = \mathrm{Tr}(\mathbf{d}\boldsymbol{\rho}), \tag{31}$$

where $\boldsymbol{\rho}$ is the ground-state one-particle matrix,

$$\rho_{sr} = \langle\Psi_0|c_r^\dagger c_s|\Psi_0\rangle, \tag{32}$$

and $\mathbf{d}$ is the matrix of one-particle integrals $d_{rs}$ [Eq. (12)]. A strictly consistent treatment of $D_0$ at the ADC(2) level would require to evaluate the density matrix through second order of perturbation theory, $\boldsymbol{\rho}(2)=\boldsymbol{\rho}^{(0)}+\boldsymbol{\rho}^{(2)}$ (note that the first-order contribution vanishes). In general, however, it is advisable to resort to an improved treatment of the ground-state density and corresponding ground-state properties (see, for example, the discussion given in Sec. II B of Ref. 28). As the method of choice we here use the so-called Dyson expansion method (DEM) based on the third-order ADC approximation [ADC(3)] for the one-particle Green's function (electron propagator). For a detailed description the reader is referred to Ref. 36 and to Sec. V A of Ref. 37. The DEM/ADC(3) approximation for the ground-state density matrix is consistent through third order of perturbation theory and considers higher-order contributions in the form of infinite partial (incomplete) summations.

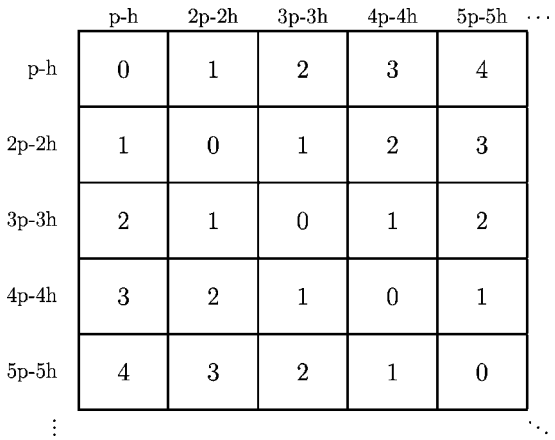


FIG. 3. Order relations for the blocks of the ADC secular matrix. The numbers in the blocks indicate the lowest nonvanishing order of perturbation theory.

## IV. ASPECTS OF THE EXCITED STATE ISR FORMULATION

The ADC approximation schemes combine the eigenvalue problem (diagonalization) of a Hermitian secular matrix and perturbation theory for the secular matrix elements. Two properties referred to as compactness and separability establish the usefulness of these methods.[34,38] The former property means that the truncation error associated with restricting the configuration space to the $\mu$ lowest excitation classes is of the order $2\mu$ (for singly excited states). The separability property, on the other hand, ensures size-consistent (size-intensive) results for excitation energies and transition moments. In Secs. IV A and IV B the corresponding properties for the excited states are discussed. A brief analysis of the dipole sum rule and the equivalence of the length and velocity forms of the transition moments in the excited state ISR formulation is given in Sec. IV C. Finally, in Sec. IV D three more aspects of the present development are addressed.

### A. Truncation error

To analyze the perturbation–theoretical consistency of systematical (classwise) truncation of the explicit configuration space, one has to inspect the so-called order relations for the quantities of interest. For example, the order relations for the ADC secular matrix are given by[34]

$$\mathbf{M}_{\mu\mu'} = O(|\mu-\mu'|), \quad \mu,\mu' = 1,2,\ldots \tag{33}$$

which means that in the matrix elements of the block $\mathbf{M}_{\mu\mu'}$ the lowest nonvanishing contributions are of the order $|\mu-\mu'|$. These "canonical" order relations[34] are shown schematically in Fig. 3. The canonical order relations for the secular matrix lead to the order relations

$$\underline{X}_\mu = O(\mu-1), \quad \mu = 1,2,\ldots \tag{34}$$

| | p-h | 2p-2h | 3p-3h | 4p-4h | 5p-5h | ⋯ |
|---|---|---|---|---|---|---|
| p-h | 0 | 0 | 1 | 2 | 3 | |
| 2p-2h | 0 | 0 | 0 | 1 | 2 | |
| 3p-3h | 1 | 0 | 0 | 0 | 1 | |
| 4p-4h | 2 | 1 | 0 | 0 | 0 | |
| 5p-5h | 3 | 2 | 1 | 0 | 0 | |
| ⋮ | | | | | | ⋱ |

FIG. 4. Order relations for the blocks of the ISR (or ADC) matrix for a single-particle operator $\hat{D}$. The numbers in the blocks indicate the lowest nonvanishing order of perturbation theory.

for the eigenvectors of singly excited states. Following the proof given in Appendix A of Ref. 34 one can easily establish the order relations

$$\mathbf{D}_{\mu\mu'}=O(|\mu-\mu'|-1), \quad |\mu-\mu'|\geqslant 1 \tag{35}$$

for the ISR of an arbitrary one-particle operator, $\hat{D}$ (see Fig. 4); the diagonal blocks ($\mu=\mu'$) are, of course, of zeroth order. Let us note that the order relations (35) are less stringent than those of the secular matrix as there is zeroth-order coupling between adjacent excitation classes. To determine the truncation errors for an excited state expectation value, $D_n$, or transition moment, $T_{mn}$, one has to consider the expression

$$T_{mn}=\underline{X}_m^{\dagger}\mathbf{D}\underline{X}_n \tag{36}$$

obtained by multiplying the ISR matrix $\mathbf{D}$ with the respective eigenvectors. Using the order relations (34), the truncation error for matrix elements $T_{mn}$ of singly excited states is seen to be $2\mu-1$, where $\mu$ is the highest explicit configuration class. More specifically, this means that at the ADC(2) level of theory ($\mu=2$) the (singly) excited state are treated consistently through second order. However, third-order consistency cannot be reached at the ADC(3) level, the explicit configuration space being here the same as in the ADC(2) case.

The analysis can readily be generalized to excited state transition moments involving one or two doubly excited states. In a similar way one can analyze the case of a two-particle operator. The results are summarized in Table I.

### B. Separability and size consistency

For the analysis of the separability property we consider, as usual, a system $S$ consisting of two noninteracting (separate) parts (fragments) $A$ and $B$. The Hamiltonian of $S$ is given by the sum

$$\hat{H}=\hat{H}_A+\hat{H}_B \tag{37}$$

of the fragment Hamiltonians $\hat{H}_A$ and $\hat{H}_B$, and the same partitioning applies to any other physical operator, i.e.,

TABLE I. Analysis of the ADC truncation error for excited state moments involving singly ($p-h$) and doubly ($2p-2h$) excited states. Given is the perturbation–theoretical order of the error resulting from truncating the expansion manifold after excitation class $\mu$; first and second line corresponds to one- and two-particle property operators, respectively.

| Operator type | $p-h/p-h$ | $p-h/2p-2h$ | $2p-2h/2p-2h$ |
|---|---|---|---|
| $1p$ | $2\mu-1$ | $2(\mu-1)$[a] | $2(\mu-1)-1$[a] |
| $2p$ | $2(\mu-1)$[a] | $2(\mu-1)-1$[a] | $2(\mu-2)$[b] |

[a]For $\mu\geqslant 2$.
[b]For $\mu\geqslant 3$.

$$\hat{D}=\hat{D}_A+\hat{D}_B. \tag{38}$$

Note that for the following considerations $\hat{D}$ needs not be restricted to be a one-particle operator. One can further assume a localized one-particle basis set, that is, the one-particle states (orbitals) are either localized on $A$ or on $B$. As a consequence, one can distinguish three classes of $N$-electron configurations, $J\equiv J_A,J_B$, and $J_{AB}$, where $J_A$ and $J_B$ denote configurations local on $A$ or $B$, respectively, while $J_{AB}$ refers to a nonlocal (or mixed) configuration involving both fragments, $A$ and $B$. To proceed let us briefly review the essential localization properties of the intermediate states.[38]

For a local configuration $J_A$ on $A$ the intermediate state is given by the product

$$|\tilde{\Psi}_{J_A}\rangle=|\tilde{\Psi}^A_{J_A}\rangle|\Psi^B_0\rangle \tag{39}$$

of the ground state of fragment $B$, $|\Psi^B_0\rangle$, and the intermediate state, $|\tilde{\Psi}^A_{J_A}\rangle$ of fragment $A$. (Note that the antisymmetrization of the total wave function is of no importance here.) An analogous expression, $|\tilde{\Psi}_{J_B}\rangle=|\tilde{\Psi}^B_{J_B}\rangle|\Psi^A_0\rangle$ applies to a local excitation on $B$. While seemingly plausible, it is a nontrivial result[38] that the product form

$$|\tilde{\Psi}_{J_{AB}}\rangle=|\tilde{\Psi}^A_{J_A}\rangle|\tilde{\Psi}^B_{J_B}\rangle \tag{40}$$

holds for the nonlocal excitations, $J_{AB}\equiv J_AJ_B$. It should be noted that this result comprises the case, where $J_A$ and $J_B$ refer to general non-neutral excitations on the respective fragments, such as ionization on $A$ and electron attachement on $B$. An immediate consequence of the product form (40) of the intermediate states is the separability property of the ADC secular matrix (see Fig. 5). Besides the fact that there is no coupling between the local configurations, i.e., $\mathbf{M}_{AB}=\mathbf{0}$, also the coupling between local and nonlocal configurations vanishes, that is, $\mathbf{M}_{A,AB}=\mathbf{M}_{B,AB}=\mathbf{0}$. Moreover, the diagonal $A$ and $B$ subblocks of $\mathbf{M}$ are identical to the fragment secular matrices, $\mathbf{M}_{AA}=\mathbf{M}^A$, $\mathbf{M}_{BB}=\mathbf{M}^B$. Obviously the resulting excitation energies are size intensive, that is, the result for a local excitation, say on $A$, is independent of whether the method is applied to the entire system or to fragment $A$.

A similar result is found for the (ground-to-excited-state) transition moment of a local excitation. The eigenvector of a local excitation $n$, say on $A$, has nonvanishing components only for configurations, $X_{J_An}$, being local on $A$. Thus, the transition moment becomes

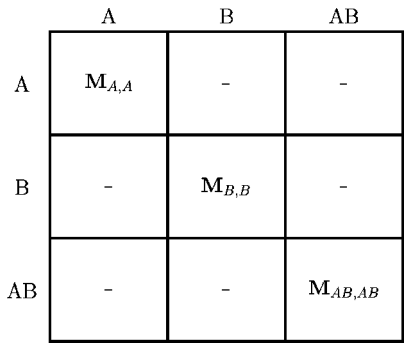


FIG. 5. Block structure of the ADC secular matrix **M** with respect to the partitioning of the configuration space into local and nonlocal configurations in a two-fragment system, $\mathbf{S}=\mathbf{A}+\mathbf{B}$.

$$T_n=\sum_{J_A} X_{J_A n}F_{J_A}, \tag{41}$$

where

$$F_{J_A}=\langle\tilde{\Psi}_{J_A}|\hat{D}|\Psi_0\rangle=\langle\tilde{\Psi}^A_{J_A}|\hat{D}_A|\Psi^A_0\rangle \tag{42}$$

is equal to the fragment ISR transition moment, $F^A_{J_A}$.

Now let us consider excited state matrix elements of a general physical operator $\hat{D}$. As a consequence of the product forms (39) and (40) the ISR matrix **D** of the subtracted operator $\hat{D}-D_0$ has the block structure shown in Fig. 6; here $D_0$ is the ground-state expectation value of $\hat{D}$. Obviously, **D** is not of the separable form as the secular matrix **M**: while there is no direct coupling of the two local blocks ($\mathbf{D}_{AB}=\mathbf{0}$), there may arise nonvanishing coupling matrix elements for local and nonlocal configurations. But this is not detrimental to matrix elements of two excited states $m$ and $n$, being both local excitations on, say, fragment $A$, because the multiplication with the corresponding eigenvectors projects out any nonlocal matrix elements:

$$T_{mn}=\underline{X}^{\dagger}_{Am}\mathbf{D}_{AA}\underline{X}_{An}. \tag{43}$$

Here $\underline{X}_{An}$ denotes the nonvanishing (local) part of the full eigenvector $\underline{X}_n$. It remains to inspect the relation of the $\mathbf{D}_{AA}$ block to the fragment ISR matrix, $\mathbf{D}^{(A)}$. A general matrix element of two local (on $A$) intermediate states,

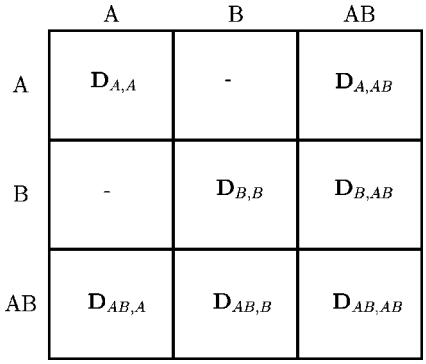


FIG. 6. Block structure of the ISR (or ADC) matrix **D** for a single-particle operator $\hat{D}$ with respect to the partitioning of the configuration space into local and nonlocal configurations in a two-fragment system, $\mathbf{S}=\mathbf{A}+\mathbf{B}$.

$$D_{I_AJ_A}=\langle\tilde{\Psi}_{I_A}|\hat{D}|\tilde{\Psi}_{J_A}\rangle-\delta_{I_AJ_A}D_0 \tag{44}$$

can be evaluated further using the product forms [Eqs. (39), and (40)] of the intermediate states to yield

$$D_{I_AJ_A}=\langle\tilde{\Psi}^A_{I_A}|\hat{D}_A|\tilde{\Psi}^A_{J_A}\rangle-\delta_{I_AJ_A}D^A_0, \tag{45}$$

where $D^A_0=\langle\Psi^A_0|\hat{D}_A|\Psi^A_0\rangle$ denotes the ground state expectation value of $\hat{D}$ for fragment $A$. Note that $D_0=D^A_0+D^B_0$. This result, which may be written more compactly as

$$\mathbf{D}_{AA}=\mathbf{D}^A \tag{46}$$

means that the local block of the ''global'' ISR matrix is identical to the fragment ISR matrix. For the ISR matrix of the original (unshifted) operator $\hat{D}$ one must consider also the diagonal $D_0$ contribution,

$$\tilde{\mathbf{D}}_{AA}=\tilde{\mathbf{D}}^A+\mathbf{1}D^B_0. \tag{47}$$

An excited state expectation value, $D_n$, computed for the entire system $S$ is the sum of the corresponding fragment ($A$) expectation value and the ground state expectation value of the other (unaffacted) fragment ($B$), as is to be expected. In the case of excited state transition moments ($m\neq n$), the global moments are equal to the fragment moments as the latter term on the right-hand side of Eq. (46) does not lead to a contribution due to the orthogonality of the excited states.

To conclude, the ISR formulation of excited state properties and transition moments is size consistent. Moreover, as can be easily seen, that property not only applies to the formally exact formulation but also to the ADC($n$) approximation schemes.

### C. Dipole sum rule and the equivalence of length and velocity forms

The well-known Thomas–Reiche–Kuhn (TRK) or dipole sum rule is usually applied to transitions from the ground state. But it may as well be formulated for the more general case where the initial state is an excited state, reading here

$$S^1_n(z)=\sum_m (E_m-E_n)|\langle\Psi_m|\hat{Z}|\Psi_n\rangle|^2=\frac{1}{2}N. \tag{48}$$

Here $\hat{Z}$ denotes the $z$ component of the dipole operator and $N$ is the number of electrons. The summation over states on the right-hand side includes the ground state ($m=0$). The sum rule (48) may serve as a test for the quality of the method used to compute the excited state energies and transition moments. For this purpose it is convenient to replace the sum-over-states expression (48) by the following compact form:

$$S^1_n(z)=\underline{X}^{\dagger}_n(\tilde{\mathbf{Z}}\mathbf{M}\tilde{\mathbf{Z}}-(E_n-E_0)\tilde{\mathbf{Z}}^2)\underline{X}_n, \quad n\neq 0. \tag{49}$$

Here $\underline{X}_n$ is the $n$th eigenvector of the ISR matrix **M**; $\tilde{\mathbf{Z}}$ and $\tilde{\mathbf{Z}}^2$ denote the ISR matrices of $\hat{Z}$ and $\hat{Z}^2$, respectively.

In a similar way, the relation between the dipole length ($L$) and dipole velocity ($V$) forms of the transition moments can be formulated for transitions between excited states. As is well known, that relation is a consequence of the operator identity,

$$[\hat{H},\hat{Z}]=-i\hat{P}_z, \tag{50}$$

where $\hat{P}_z$ is the $z$ component of the momentum operator. For the transition between the excited states $m$ and $n$ one obtains the explicit relations

$$(E_n-E_m)\langle\Psi_n|\hat{Z}|\Psi_m\rangle=-i\langle\Psi_n|\hat{P}_z|\Psi_m\rangle, \tag{51}$$

which in turn can be transformed into the following global identity:

$$\mathbf{M}\tilde{\mathbf{Z}}-\tilde{\mathbf{Z}}\mathbf{M}=-i\tilde{\mathbf{P}}_z \tag{52}$$

which is independent of the individual transitions. Here $\tilde{\mathbf{P}}_z$ is the ISR matrix of $\hat{P}_z$.

### D. Other features

A useful test of the explicit ISR expressions is provided by the special case of the particle-number operator,

$$\hat{N}=\sum_r c_r^\dagger c_r. \tag{53}$$

Since the intermediate states are eigenfunctions of $\hat{N}$, the ISR matrix elements are of the form

$$\langle\tilde{\Psi}_I|\hat{N}|\tilde{\Psi}_J\rangle=N\delta_{IJ}. \tag{54}$$

These relations must be fulfilled (in each order) by the perturbation–theoretical expressions for the special choice, $d_{rs}=\delta_{rs}$, of the one-particle matrix elements. Of course, this test pertains only to those terms involving diagonal one-particle elements, $d_{pp}$.

Let us next consider the ISR of the operator product $\hat{A}\hat{B}$ of two physical operators $\hat{A}$, $\hat{B}$,

$$\begin{aligned}(\hat{A}\hat{B})_{IJ}&=\langle\tilde{\Psi}_I|\hat{A}\hat{B}|\tilde{\Psi}_J\rangle\\&=\langle\tilde{\Psi}_I|\hat{A}|\Psi_0\rangle\langle\Psi_0|\hat{B}|\tilde{\Psi}_J\rangle+\sum_K\langle\tilde{\Psi}_I|\hat{A}|\tilde{\Psi}_K\rangle\\&\quad\times\langle\tilde{\Psi}_K|\hat{B}|\tilde{\Psi}_J\rangle.\end{aligned} \tag{55}$$

Here the last line is obtained by inserting the ISR resolution of identity, $|\Psi_0\rangle\langle\Psi_0|+\Sigma_K|\Psi_K\rangle\langle\Psi_K|=\hat{1}$. This result can be written in the form

$$(\hat{A}\hat{B})_{IJ}=F_I(A)F_J(B)^*+(\tilde{\mathbf{A}}\tilde{\mathbf{B}})_{IJ}, \tag{56}$$

where $F_I(A)=\langle\Psi_I|\hat{A}|\Psi_0\rangle$ is the (ground state) ISR transition moment for the operator $\hat{A}$ and $\tilde{\mathbf{A}}$, $\tilde{\mathbf{B}}$ denote the corresponding ISR matrices. If $\hat{A}$ and $\hat{B}$ are one-particle operators, the ISR of the product $\hat{A}\hat{B}$ can readily be evaluated at the ADC(2) level using the ADC(2) expressions for ground-state transition moments [Eqs. (B1)–(B13) in Ref. 25] and the second-order ISR expressions given in the Appendix.

The present ISR development allows one to extend the original Hamiltonian $\hat{H}$ (underlying the generation of the intermediate states) by an arbitrary one-particle operator, $\hat{U}$, representing, for example, an external potential: $\hat{H}\rightarrow\hat{H}^x=\hat{H}+\hat{U}$. Because the (excited) intermediate states now may couple to the ground state, the IS configuration space must be enlarged by $|\Psi_0\rangle$. The additional ISR secular matrix elements read

$$M^x_{00}=U_0,\quad M^x_{I0}=\langle\tilde{\Psi}_I|\hat{U}|\Psi_0\rangle=F_I(U),\quad I\neq 0, \tag{57}$$

where the subscript 0 refers to the ground state and $F_I(U)$ are the ISR ground-to-excited-state transition moments for the operator $\hat{U}$. The matrix elements in the excited state block are obtained by adding the ISR matrix of $\hat{U}$ to the original secular matrix $\mathbf{M}$:

$$M^x_{IJ}=M_{IJ}+\tilde{U}_{IJ},\quad I,J\neq 0. \tag{58}$$

It should be noted that for a parameter dependent operator, $\hat{U}=\hat{U}(\lambda)$, the Hellmann–Feynman relation is valid in the form

$$\frac{d}{d\lambda}E_n(\lambda)=\underline{Y}_n^\dagger(\lambda)\tilde{\mathbf{U}}'(\lambda)\underline{Y}_n(\lambda), \tag{59}$$

where $\tilde{\mathbf{U}}'$ is the extended ISR matrix of $(\partial/\partial\lambda)\hat{U}$ and $\underline{Y}_n$ denotes the $n$th eigenvector of the extended secular matrix, $\mathbf{M}^x$. In the special case, $\hat{U}(\lambda)\rightarrow\lambda\hat{U}$, the energy derivatives at $\lambda=0$ simply become

$$\left.\frac{d}{d\lambda}E_n\right|_{\lambda=0}=\underline{X}_n^\dagger\tilde{\mathbf{U}}\underline{X}_n,\quad n\neq 0 \tag{60}$$

that is, excited state expectation values of $\hat{U}$. The latter equation provides the starting point for analytical ES energy derivatives in the case of fixed (''unrelaxed'') HF orbitals.

## V. COMPUTATIONS

### A. Coding of the properties ISR

An excited state properties code at the ADC(2) level of approximation was written as an extension of the existing ADC(3) program[28] for electron excitation. The major new parts are routines required for the evaluation of the property ISR matrix elements, that is, zeroth- and second-order terms in the $p-h$ diagonal block, $\mathbf{D}_{11}$, zeroth- and first-order terms in the $p-h/2p-2h$ coupling blocks, $\mathbf{D}_{12}$, and zeroth-order terms in the $2p-2h$ diagonal block, $\mathbf{D}_{22}$. In addition to orbital energies and Coulomb integrals, the one-particle integrals, $d_{rs}$, of the considered property operator, $\hat{D}$, are required as input data for these matrix elements.

Before coding, the explicit spin–orbital expressions for the ISR property matrix elements (as given in the Appendix) had to be written in a form exploiting the underlying spin (and spatial) symmetry properties of the matrix elements. Assuming a spin-independent property operator, spin-free working equations were derived using standard angular momentum algebra techniques. In a first step, the property ISR matrix is transformed from the original spin–orbital (or ''primitive'') form to a representation associated with spin-adapted singlet ($S=0$) and triplet ($S=1$) intermediate states. In this spin-adapted form the ISR matrix is decoupled with respect to $S=0$ and 1; moreover, the triplet block decomposes into three equal $M_S$ subblocks, $M_S=1,\ 0,\ -1$. Subsequently, the spin summations in the perturbation–

TABLE II. Full CI and Hartree–Fock (HF) results for the ground-state energies and dipole moments of the $H_2O$ and HF molecules using the 3-21G basis set; dipole moments have been computed also at the levels of second order of perturbation theory [PT(2)] and the Dyson expansion method (DEM) (see text).

| | Ground-state energy (a.u.) | | Dipole moment ($D$) | | | |
|---|---|---|---|---|---|---|
| Molecule | FCI | HF | FCI | HF | PT(2) | DEM |
| $H_2O$ | −75.714 959 | −75.585 378 | −2.30 | −2.44 | −2.36 | −2.32 |
| HF | −99.584 768 | −99.459 752 | 2.03 | 2.16 | 2.08 | 2.04 |

theoretical expressions can be performed, yielding the desired spin-free expressions for the ISR matrix elements. The generation of the spin-free expressions was done in a semiautomatic way using a specially devised computer program. Spatial symmetry reductions are considered in the present code only to the extent of Abelian groups or subgroups, having only one-dimensional irreducible representations.

In devising the present prototypical ISR property code, emphasis was laid on an utmost secure and error-free realization rather than on efficiency. The development of a follow-up program aiming at higher efficiency is the logical next step.

An obvious example for the need of improvement is the strategy used to perform the matrix×vector (MV) product, $\mathbf{D}\underline{X}_n$, in the evaluation of Eqs. (22) and (24). In the present program version, the $\mathbf{D}$ matrix elements are evaluated once and then the MV product is formed. The computational bottleneck here is the $p-h$ diagonal block, $\mathbf{D}_{11}$, having $\sim N^4$ nonvanishing matrix elements, where $N$ denotes the number of orbitals. As the evaluation of each of its matrix elements scales as $N^3$ the overall cost for computing $\mathbf{D}_{11}$ scales as $N^7$. A more advantagous technique would be to break the MV product into intermediate quantities obtained by multiplying the eigenvector components with suitable parts of the second-order expressions for the $\mathbf{D}_{11}$ matrix elements (for a similar procedure see Sec. III A of Ref. 28). Using such techniques the scaling behavior of the property part at the ADC(2) level reduces to $N^5$.

The present ADC code is interfaced to the GAMESS[39] *ab initio* program package generating the HF input data [orbital energies, one and two-electron molecular orbital (MO) integrals] for the ensuing ADC calculations.

### B. Comparison with full CI results

For a first test and validation of the present development we have performed both ADC and full configuration–interaction (FCI) computations for the $H_2O$ and HF molecules at the small 3-21G[40] AO basis set level. The FCI computations were done with the determinantal FCI code[41] of the GAMESS program package.[39] The following geometrical parameters were used: $R_{OH}=0.957$ Å, $\angle$HOH $=104.5°$, $R_{HF}=0.917$ Å. In both the FCI and ADC computations the $1s$ core orbitals were kept frozen. The largest dimension of the FCI space was 245 025 (for the $H_2O$ excitations at $C_1$ symmetry).

Table II collects the computed ground-state energies and dipole moments ($z$ component), $D_0(z)$. For the dipole moments, the HF and FCI results can be compared to the values obtained by evaluating Eq. (31) using the strict second-order [PT(2)] expansion for the ground-state one-particle matrix, $\boldsymbol{\rho}$, and the DEM/ADC(3) treatment, respectively. For both molecules the PT(2) and DEM results differ only slightly, the latter being in excellent agreement with the FCI values. It should be emphasized, however, that, in general, the PT(2) approximation for $D_0$ will be less satisfactory than in the

TABLE III. FCI and ADC results for (vertical) excitation energies (eV) and excited state dipole moments of $H_2O$ and HF. The ADC excitation energies are given relative to the FCI values.

| | | Excitation energies (eV) | | | | Excited state dipole moments ($D$) | | | |
|---|---|---|---|---|---|---|---|---|---|
| State/transition | | FCI | ADC(1) | ADC(2) | ADC(3) | FCI | ADC(1) | ADC(2) | ADC(3/2) |
| $H_2O$ $1\,^1A_1\rightarrow$ | | | | | | | | | |
| $1\,^1B_1$ | $1b_1-a_1$ | 8.75 | 0.90 | 0.07 | 0.02 | 0.17 | 0.76 | 0.35 | 0.24 |
| $1\,^1A_2$ | $1b_1-b_2$ | 10.95 | 0.61 | 0.12 | −0.01 | −0.19 | 0.27 | 0.01 | −0.15 |
| $2\,^1A_1$ | $3a_1-a_1$ | 11.44 | 0.80 | 0.02 | −0.01 | 0.50 | 1.15 | 0.72 | 0.60 |
| $1\,^1B_2$ | $3a_1-b_2$ | 13.77 | 0.50 | 0.11 | −0.11 | 0.24 | 0.64 | 0.45 | 0.26 |
| $2\,^1B_2$ | $1b_2-a_1$ | 16.02 | −0.02 | 0.08 | −0.15 | −0.54 | −0.24 | −0.44 | −0.52 |
| $1\,^3B_1$ | $1b_1-a_1$ | 7.90 | 0.67 | 0.02 | 0.01 | 0.15 | 0.69 | 0.32 | 0.22 |
| $1\,^3A_1$ | $3a_1-a_1$ | 10.20 | 0.22 | −0.02 | −0.05 | 0.59 | 0.80 | 0.68 | 0.61 |
| $1\,^3A_2$ | $1b_1-b_2$ | 10.37 | 0.45 | 0.09 | −0.01 | −0.12 | 0.22 | 0.03 | −0.08 |
| $1\,^3B_2$ | $3a_1-b_2$ | 12.29 | −0.13 | 0.00 | −0.04 | 0.37 | 0.32 | 0.42 | 0.39 |
| HF $1\,^1\Sigma^+\rightarrow$ | | | | | | | | | |
| $1\,^1\Pi$ | $1\pi-\sigma$ | 10.94 | 0.88 | 0.03 | 0.02 | −1.80 | −2.42 | −2.07 | −1.84 |
| $1\,^1\Sigma^+$ | $3\sigma-\sigma$ | 16.69 | 0.67 | 0.03 | −0.05 | −1.28 | −2.13 | −1.66 | −1.31 |
| $1\,^3\Pi$ | $1\pi-\sigma$ | 10.21 | 0.63 | −0.03 | 0.01 | −1.82 | −2.34 | −2.06 | −1.87 |
| $1\,^3\Sigma^+$ | $3\sigma-\sigma$ | 13.46 | −0.44 | −0.06 | −0.03 | −1.65 | −1.54 | −1.68 | −1.65 |

present case. An example, where the PT(2) approximation fails, is the CO molecule. At the FCI level using a minimal basis set (STO-3G[40]) the ground-state dipole moment is found to be $-0.63D$. Here the DEM result ($-0.67D$) gives a very good approximation, whereas the PT(2) value of $-1.30D$ is grossly off the mark. In the ensuing calculations of the excited state dipole moments the DEM/ADC(3) results for the $D_0(z)$ contributions are used throughout.

In Table III the excitation energies and dipole moments are listed of some low-lying excited singlet and triplet states of $H_2O$ and HF as computed at the FCI and different ADC levels. As for the excitation energies, the reader is referred to a recent more comprehensive study[28] of the performance of the ADC methods, where—at a distinctly better AO basis set level—also the $H_2O$ and HF molecules have been addressed. In the present small basis set computations the ADC(2) and ADC(3) results are rather similar and the deviations from the FCI excitation energies are well below the average ADC(3) error of 0.2 eV found in the larger study.

For the excited state dipole moments, the FCI results in Table III are compared to the results of three distinct ADC treatments. At the lowest level, referred to as ADC(1), the ADC eigenvectors (having only $p-h$ components) are combined with the zeroth-order ISR property matrix, that is, $\mathbf{D}_{11}^{(0)}$ (note that the first-order contributions to the $p-h$ diagonal block vanish). The ADC(1) results in Table III are seen to differ quite substantially from the FCI values, which indicates that the ADC(1) scheme is hardly a useful approximation. A distinctly improved description is obtained at the ADC(2) level, where the full ADC(2) property matrix as derived here is used together with the ADC(2) eigenvectors of the electronic excitation problem. The role of the eigenvectors in the computation of excited state properties can be seen by comparing the ADC(2) dipole moments to the results obtained by combining the ADC(2) property matrix with the eigenvectors of the ADC(3) secular matrix. These ADC(3/2) results (last column of Table III) agree indeed extremely well with the FCI standard, the mean absolute and the maximal deviation being $0.04D$ and $0.1D$, respectively, for the manifold of states listed in Table III. The good accuracy record of the ADC(3/2) results suggests that the quality of the ADC(2) property matrix itself is very satisfactory and the errors in the excited state properties at the ADC(2) level will be mainly due to insufficiencies of the ADC(2) eigenvectors.

## VI. APPLICATION TO PARANITROANILINE

As a test of greater practical importance, we have performed ADC(2) calculations for the lowest excited singlet and triplet states of the paranitroaniline (PNA) molecule (see Fig. 7). PNA is a prototypical ''push–pull'' chromophore, having a donor ($NH_2$) and an acceptor ($NO_2$) group connected by the conjugated $\pi$ system of the phenyl ring. Characteristic for such a system is the occurrence of strong intramolecular charge transfer upon electronic excitation, giving rise to extraordinary linear and nonlinear optical response properties.[42–53] The excitation induced charge transfer will also be reflected in a substantial change of the excited state dipole moments. In the prominent $2\,^1A_1$ excitation, for example, the dipole moment of PNA increases from the already large ground state value of $\sim 6D$ to about $14-15\ D$.[42,43] Clearly, the latter property renders PNA an interesting test case for the present ISR property method.

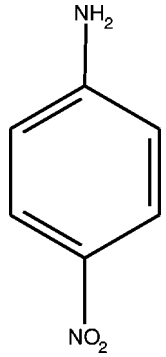


FIG. 7. The structure of paranitroaniline (PNA).

In the present computations, the ground-state geometrical parameters of PNA were optimized using DFT at the level of the B3LYP functional[54,55] and the cc-pVDZ basis set[56] (six-component representation of *d* functions). The optimization was carried out using the GAUSSIAN program package.[57] ADC calculations were performed both at the ADC(1) and ADC(2) level using the 6-31G basis set[58] and the DFT nuclear conformations. A characterization of the highest occupied and lowest unoccupied MOs is given in Table IV. In the ADC(2) calculations the *K*-shell orbitals were kept frozen. The dimension of the ADC secular matrices ranged from 332 700 ($^1A_2$) to 592 445 ($^3A_1$). Complementing calculations were performed at the ADC(1) level to check for basis set limitations and conformational effects (see below). Moreover, the singlet excitations were computed also at the extended ADC(2) level (see Ref. 28) in order to have a further check of the admixtures of doubly excited configurations. The extended ADC(2) calculations were carried out in a direct mode avoiding the storage of the large first-order part, $\mathbf{M}_{22}$, of the secular matrix.

As our ground-state calculations (see Table V) predict, the symmetric $C_{2v}$ conformation of PNA is not a stable stationary point, but rather a transition state separating two equivalent $C_s$ structures associated with a nonplanar configuration of the amino group. In view of the rather small stabi-

TABLE IV. Orbital energies (eV) and MO assignment for the 6-31G HF results.

| MO | $-\epsilon$ [eV] | Notation | Character (atomic localization) |
|---|---|---|---|
| Occupied | | | |
| $4b_1$ | 8.78 | $\pi_6$ | C(nitro)/C–C(amino)/N(amino) |
| $2a_2$ | 10.12 | $\pi_5$ | C–C(benzene) |
| $1a_2$ | 11.77 | $n(\pi)$ | O(lone pair) |
| $3b_1$ | 13.04 | $\pi_4$ | N(amino)/C–C(amino) |
| $11a_1$ | 13.05 | $\sigma$ | O/C–N(nitro) |
| $9b_2$ | 13.08 | $n(\sigma)$ | O(lone pair) |
| Virtual | | | |
| $5b_1$ | | $\pi$ | nitro/benzene |
| $3a_2$ | | $\pi$ | C–C–C–C (benzene, antibonding) |
| $6b_1$ | | $\pi$ | nitro/benzene/amino |

TABLE V. Ground state energy $E$ (a.u.), ZPVE correction (a.u.), and dipole moment ($D$) for the $C_{2v}$ and $C_s$ stationary points of PNA as obtained at the B3LYP and HF level of theory using the cc-pVDZ, 6-31G, and 6-31G+ basis sets.

| Structure | $E$ | $\|\mu\|$[a] | ZPVE | $E$+ZPVE |
|---|---|---|---|---|
| B3LYP/cc-pVDZ/optimized geometry | | | | |
| $C_{2v}$ | −492.154 617 | 7.4 | 0.118 772 | −492.035 845 |
| $C_s$[b] | −492.155 206 | 6.9 | 0.119 545 | −492.035 661 |
| HF/6-31G/B3LYP geometry | | | | |
| $C_{2v}$ | −488.990 308 | 8.1[c] | | |
| $C_s$ | −488.986 764 | 7.6 | | |
| HF/6-31G+/B3LYP geometry | | | | |
| $C_{2v}$ | −488.008 056 | 8.1 | | |
| $C_s$ | −488.004 779 | 7.6 | | |

[a]Expt. value 6.3$D$ (Ref. 48).
[b]Angle between C–N and the bisector of $NH_2$: 34.5°.
[c]Result of DEM/ADC(3) method: 7.2$D$.

lization energy, being only 3.7 kcal/mol, the out-of-plane distortion, predicted to be 34.5°, is remarkably large. In fact, the $C_s$ minima are very shallow and not stable if zero-point vibrations are taken into account. In the latter case, our calculations find that the $C_{2v}$ structure of PNA is by 1.2 kcal/mol below the nonplanar $C_s$ configurations. In any case, the nonplanarity of the PNA ground state hardly affects the ground and excited state energies, and it should be legitimate to set out from the more symmetrical $C_{2v}$ conformation in the present vertical electronic computations. The ADC(1) results given in Table VI show that the $C_{2v}$ and $C_s$ excitation energies are almost identical. Obviously, the dipole moments are more sensitive to the nuclear conformation. Here both the ground and excited state dipole moments at the $C_s$ conformation are somewhat below the corresponding $C_{2v}$ values, the differences being in the range of 0.4–0.7 $D$. It should be noted that the $C_{2v}$ structure was the preferred choice in previous theoretical work on PNA.[44,46,47,51,53,59]

To check the adequacy of the relative small 6-31G basis set (basis $A$) for the description of the lowest valence-type excitations in PNA we compare in Table VI the ADC(1) results using basis $A$ with those obtained using the somewhat larger 6-31G+ basis set[58,60] (basis $B$) containing a set of diffuse $s$ and $p$ functions. Concerning the excitation energies, a noticeable basis set effect is seen only for the third and fourth state in Table VI, for which the diffuse functions lead to an energy lowering of about 0.2 eV. As seen in Table VI, also the dipole moments are little affected by enlarging the basis, the maximal change being 0.2$D$ for the $2\,^1A_1$ state. From these results we may conclude that the 6-31G basis $A$ should essentially be adequate to treat the lowest four excited singlet states and their triplet counterparts.

The ADC(2) results for the excitation energies, oscillator strengths, and dipole moments of the four lowest excited singlet states (S1–S4) are presented in Table VII. The inspection of the eigenvectors shows that these states are characterized as single excitations [the admixture of doubly excited configurations at the extended ADC(2) level is in the range of 16–18 %]. The lowest two singlet states, $2\,^1A_2(n-\pi^*)$ and $1\,^1B_1(\sigma-\pi^*)$, are dipole forbidden or have an extremely small oscillator strength, respectively, so that it will be difficult to observe them in an ordinary photon absorption spectrum. The dominant role in the low-energy excitation regime is played by the third excited singlet state, $2\,^1A_1$, corresponding to $\pi-\pi^*$ excitation and associated with a large charge transfer (CT). The oscillator strength for the transition to the S3 CT state is 0.392 as computed at the ADC(2) level. Due to its paramount spectral strength, the $2\,^1A_1$ state has often (incorrectly) been referred to as S1. The computed vertical excitation energy (4.55 eV) for the $2\,^1A_1$ state is in good agreement with the maximum (4.25 eV) of the broad absorption band in the gas phase spectrum of Farztdinov *et al.*[50] The calculated transition dipole moment for the $2\,^1A_1$ state is 5.2$D$, which should be compared to the experimental value of 4.4$D$.[48] Slightly above the S3 state our computations predict a further $\pi-\pi^*$ excitation, $1\,^1B_2$, however, having a much smaller oscillator strength than the S3 state.

The results for the four lowest triplet excitations (T1–T4) are given in Table VIII. Obviously, their energetical order deviates from that of the corresponding singlet states. While S1,T1 and S3,T3 are related singlet–triplet pairs, and T4 corresponds to S2, there is no match for T2 and S4 among the four lowest singlet and triplet states, respectively. Most remarkable is the appearance of the $n(\pi)-\pi^*$ triplet excitation, $1\,^3B_2$, at the second position (T2) in the triplet spectrum. At the ADC(1) level (basis $A$) a corresponding singlet state is found as the fifth root at 7.00 eV. The comparison to the ADC(1) energy of the T2 state (Table VIII) reveals a very large (first-order) singlet–triplet splitting of about 4.5 eV.

Whereas various theoretical studies have been devoted to the linear and nonlinear optical properties of PNA[44–47,50,53,59] dealing, in particular, with the strong solvent dependence of these properties,[46,47,50,53,59] the theoretical work on the electronic excitations in PNA appears to be

TABLE VI. ADC(1) results for the vertical excitation energies $\Omega$ (eV) and dipole moments $|\mu|$ ($D$) of the lowest excited singlet states of PNA in the $C_{2v}$ and $C_s$ conformations using the 6-31G($A$) and 6-31G+($B$) basis sets.

| State/transition | | | $\Omega(C_{2v})$ | | $\|\mu(C_{2v})\|$ | | $\Omega(C_s)$ | $\|\mu(C_s)\|$ |
|---|---|---|---|---|---|---|---|---|
| $C_{2v}$ | $C_s$ | | $A$ | $B$ | $A$ | $B$ | $A$ | $A$ |
| $1\,^1A_2$ | $1\,^1A''$ | $n(\sigma)-\pi^*$ | 4.82 | 4.79 | 5.7 | 5.7 | 4.80 | 5.3 |
| $1\,^1B_1$ | $2\,^1A'$ | $\sigma-\pi^*$ | 5.03 | 5.01 | 6.3 | 6.4 | 5.02 | 5.9 |
| $2\,^1A_1$ | $3\,^1A'$ | $\pi_6-\pi^*$ | 5.44 | 5.23 | 14.3 | 14.5 | 5.49 | 13.6 |
| $1\,^1B_2$ | $2\,^1A''$ | $\pi_6-\pi^*$ | 5.91 | 5.75 | 10.6 | 10.6 | 5.92 | 10.2 |

TABLE VII. Vertical excitation energies $\Omega$ (eV), dipole moments $|\mu|$ ($D$), and oscillator strengths of the lowest excited singlet states of PNA as obtained at the ADC(2) and ADC(1) level of theory using the 6-31G basis set.

| State/Transition | | S/D[a] | ADC(1) $\Omega$ | ADC(1) $\lvert\mu\rvert$ | ADC(2) $\Omega$ | ADC(2) $\lvert\mu\rvert$ | $f$ |
|---|---|---|---|---|---|---|---|
| $1\,^1A_2$ (S1) | $n(\sigma)-\pi^*$ | 84/16 | 4.82 | 5.7 | 3.84 | 4.9 | |
| $1\,^1B_1$ (S2) | $\sigma-\pi^*$ | 84/16 | 5.03 | 6.3 | 4.35 | 5.1 | $<0.001$ |
| $2\,^1A_1$ (S3) | $\pi_6-\pi^*$ | 82/18 | 5.44 | 14.3 | 4.55[b,c] | 17.0[d] | 0.392 |
| $1\,^1B_2$ (S4) | $\pi_{5,6}-\pi^*$ | 83/17 | 5.91 | 10.6 | 4.88 | 9.0 | 0.011 |

[a]Percentage of single (S) and double (D) excitations in the eigenvectors of the extended ADC(2) version.
[b]Expt. value (absorption maximum in vapor): 4.25 eV (Ref. 50).
[c]CASPT2 result: 3.80 eV (Ref. 59).
[d]CASPT2 result: 17.3$D$ (Ref. 59).

rather scarce. Serrano-Andrés *et al.*[59] have performed large-scale CASPT2 calculations on PNA excitations, but they report only results for the CT state (see Table VIII). The CASPT2 result for the excitation energy of the CT state is 0.75 eV below the present ADC(2) value. Discrepancies of that magnitude between CASPT2 and other results, including ADC(2), have been found previously for $\pi-\pi^*$ excitation energies in several molecules,[61–64] and there is an ongoing debate on that issue. Compared to the experimental (gas phase) result of Farztdinov *et al.*,[50] the CASPT2 value is 0.45 eV too low, whereas the present ADC(2) result overshoots by 0.3 eV. The random phase approximation (RPA) and multiconfiguration self-consistent field (MCSCF) was used in a series of PNA response properties studies,[45–47] disclosing again only the results for the CT state. The RPA and MCSCF values of 5.04 eV and 5.18 eV, respectively, reported here (see Mikkelsen *et al.*[46]) appear much too large. More recently, Salek *et al.*[51] and Moran *et al.*[53] have carried out time-dependent density functional theory (TDDFT) computations of the lowest singlet excitations in PNA, apparently yielding very satisfactory results for the excitation energy (4.13 eV and 4.07 eV, respectively) and the oscillator strength (0.332 and 0.313, respectively) of the CT state. Unfortunately, for other states the comparison to the TDDFT results is impeded by the instance that neither symmetry nor orbital specifications have been given. One may also consult recent semiempirical results obtained by Farztdinov *et al.*[50] using the SAM1 (semi ab initio model).[65] In spite of an incidental coincidence of the excitation energies for the S1 and the CT states and the corresponding ADC(2) values, little consistency is seen between the SAM1 and our results. For example, the SAM1 calculation places the CT state energetically at the fourth position (S4) and assigns it to the $^1B_1$ symmetry species. As far as the triplet states are concerned, we are not aware of any previous *ab initio* calculations.

TABLE VIII. Low-lying triplet states of PNA: ADC(2) and ADC(1) results (6-31G basis set) for vertical excitation energies $\Omega$ (eV) and dipole moments $|\mu|$ ($D$).

| State/Transition | | ADC(1) $\Omega$ | ADC(1) $\lvert\mu\rvert$ | ADC(2) $\Omega$ | ADC(2) $\lvert\mu\rvert$ |
|---|---|---|---|---|---|
| $1\,^3A_2$ (T1) | $n(\sigma)-\pi^*$ | 4.21 | 5.7 | 3.55 | 4.9 |
| $1\,^3B_2$ (T2) | $n(\pi)-\pi^*$ | 2.44 | 5.5 | 3.65 | 4.5 |
| $1\,^3A_1$ (T3) | $\pi_6-\pi^*$ | 3.38 | 9.0 | 3.73 | 11.7 |
| $1\,^3B_1$ (T4) | $\sigma-\pi^*$ | 4.44 | 6.4 | 4.11 | 5.2 |

Let us finally take a look at the excited state dipole moments listed in Tables VII and VIII, respectively. Most conspicuous is, of course, the large dipole moment of the S3 state reflecting clearly a large intramolecular charge transfer accompanying the $\pi_6-\pi^*$ excitation. As is well known, the excited S3 state corresponds to a zwitterionic, quinoid structure of the molecule, the amino and nitro groups bearing formal charges of $+e$ and $-e$, respectively. The (classical) dipole moment of such a structure is easily estimated to be in the order of 30$D$. The computed (vertical) dipole moment of 17.0$D$, being in good agreement with the corresponding CASPT2 value[59] of 17.3$D$, may be somewhat too large. As can be seen at the ADC(1) level (Table VI), a reduction in the order of 0.7$D$ may result if the dipole moment is computed at the $C_s$ conformation rather than at $C_{2v}$. As was discussed in Sec. V, the computed dipole moments depend quite sensitively on the quality of the ADC eigenvectors. Replacing the ADC(2) eigenvector by that of the extended ADC(2) level gives a somewhat smaller value (16.0$D$), and an even further reduction of the S3 dipole moment might result if the ADC(3) eigenvector could be used.

Interestingly, the T3 triplet counterpart to the CT singlet state, S3, has a distinctly smaller dipole moment, 11.7$D$, according to the present results. This indicates that apart from the spin multiplicities these states differ also to some extent with respect to their charge distributions.

Experimental dipole moments for the singlet excited CT state of PNA in different solutions, lying in the range of 14–15 $D$, have been reported, among others, by Liptay[43] and Wortmann *et al.*[48] An experimental value of 11$D$ was estimated by Schuddeboom *et al.*[49] for the ''pure'' $^3\pi-\pi^*$ state. It should be clear, however, that one must be very cautious when comparing the theoretical results with experimental data. Besides the solvent effects not accounted for in the present theory, the theoretical dipole moments are static quantities computed for the ground-state conformation of the molecule, which means that any effects associated with the nuclear motion of the electronically excited molecule are disregarded. For PNA it is known that a complex nuclear dynamics is triggered upon excitation of the CT state (see, for example, Schuddeboom *et al.*[49]), involving intersystem crossing (ISC) and possibly also internal conversion (IC)

processes. In view of the present results, predicting four triplet states, T1–T4 (and two singlet states, S1 and S2), below the CT singlet state populated in photoabsorption, it is by no means clear how the experimental signal can be attributed to a distinct excited state so that previous experimental assessments have to be reconsidered.

## VII. CONCLUSIONS

The ISR reformulation of the ADC propagator method allows for a direct approach to excited state wave functions and properties, thereby overcoming certain constraints of the original propagator formalism. The concept is based on a well-defined construction procedure (basically Gram–Schmidt orthogonalization of successive excitation classes) transforming the so-called ''correlated'' excited states, i.e. states obtained by applying HF excitation operators to the exact (correlated) ground state, into a complete set of intermediate states. These intermediate states define a Hermitian matrix representation of the Hamiltonian, referred to as ADC secular matrix, which is amenable to perturbation–theoretical expansions at successively higher levels of consistency [ADC($n$) approximations]. Solving the eigenvalue problem of the ADC secular matrix gives access to the (excitation) energies in the form of the eigenvalues; combined with the intermediate basis states, the eigenvectors form an explicit representation of the excited states. In this work the ISR concept has been extended to the representation of an arbitrary one-particle (property) operator, which is required for evaluating ES properties and moments from the IS basis expansion of excited states. More specifically, the explicit ISR property matrix has been constructed and implemented at the second order or ADC(2) level of theory. In combination with ADC(2) or ADC(3) eigenvectors, this leads to a consistent second order treatment of ES properties and moments for singly excited states. First test calculations presented here indicate that especially the ADC(3/2) scheme using the ADC(3) eigenvectors gives very satisfactory results.

From a methodological point of view, the ADC approximations combine diagonalization (of a secular matrix) and perturbation theory (for the elements of the secular and property matrices). The ISR formulation makes apparent that—apart from the possible subtraction of the ground state energy, $E_0$, in the diagonal of the secular matrix—perturbation theory comes into play only in the construction of the intermediate states, being completely determined by the exact ground state and the underlying basis of one-particle states (HF orbitals). This means that the perturbation expansions for the various ADC matrices are entirely based on the perturbation theory for the ground state. As a consequence, the convergence behavior of the ADC expansions is similar to that of the the ground state perturbation theory. This has been termed the regularity of the ADC perturbation expansions.

The usefulness of the ADC method is based on two basic features, refered to as separability and compactness. The separability (of the secular matrix) guarantees size-consistent (more precisely, size intensive) results for excitation energies and GS transition moments. As the present analysis has shown, the size consistency pertains as well to the excited state properties and transition moments. This means, for example, that in a system consisting of noninteracting fragments the total dipole moment of a locally excited state is obtained as the sum of the dipole moment of the excited fragment and the ground-state dipole moments of the other fragments. The compactness, on the other hand, means that the truncation error arising from restricting the IS expansion manifold to the lowest, say $\mu$, excitation classes is minimal. In the case of the ES properties and moments the truncation error (for singly excited states) is of the order $2\mu-1$, which is to be compared with the $2\mu$ truncation error for the excitation energies and the GS transition moments.

Another option offered by the present development is the possibility to augment the ADC secular matrix by the ISR of an arbitrary one-particle operator, say, an ''external'' potential $\hat{U}$. This allows one to treat the secular problem of the extended Hamiltonian, $\hat{H}+\hat{U}$, in a very simple and appealing way. An important aspect here is that the IS manifold itself, being based entirely on the ground state, can be kept as constructed for the original Hamiltonian, $\hat{H}$. This is reflected by the form of the additional part of the secular matrix, being, of course, linear in the external potential $\hat{U}$. More generally speaking, the ISR approach introduces a clear distinction between the treatment of the ground state and the corresponding construction of the intermediate states, on the one-hand side, and the final state problem, on the other hand. In principle, one could use completely different Hamiltonians for either part of the problem. In the usual propagator formalism, by contrast, ground and final state aspects are entangled in a hardly separable way, as can be seen, for example, in their diagrammatic perturbation expansions. Introducing an additional external potential $\hat{U}$ leads inevitably to diagrams corresponding to higher orders in $\hat{U}$, and there is no *a priori* procedure for distinguishing ground and final state contributions.

It should be noted that the present development also lays the foundation for an ADC formulation of higher response properties of molecules in the ground state. Using the ISR property matrices, one can easily recast the exact response functions into closed-form ADC expressions, which so far was possible for the linear response only.

Of course, the property ISR concept, developed here for (neutral) electronic excitations, can readily be generalized to other cases, such as (single-electron) ionization or electron attachment. In the former case, for example, the IS states are constructed from ''correlated'' ionic states formed by the action of HF ionization operators on the exact (neutral) ground state. For more details of the ISR formulation of the ionization part of the electron propagator, also referred to as non-Dyson ADC method, the reader is refered to Ref. 35; explicit expressions for the ionic property ISR at the ADC(2) level will be presented in a forthcoming publication.[66]

To summarize, the ISR property extension of the ADC propagator method is a conceptually simple approach to properties of molecules in excited states. Maintaining the advantages of propagator theory, one gains the full flexibility of a wave function description. The approximative ADC(2) level worked out here should prove a practical and suffi-

ciently accurate means of computation of ES properties and transition moments, being of particular interest for the treatment of larger molecules, as the present exploratory study of the PNA excitations may have demonstrated. Based on a more efficient program version, we hope to be able to present further tests of the method in the near future.

## ACKNOWLEDGMENT

This work has been supported by a grant of the Deutsche Forschungsgemeinschaft (DFG).

## APPENDIX: SECOND-ORDER INTERMEDIATE STATE REPRESENTATION OF A GENERAL ONE-PARTICLE OPERATOR

In the following we collect the explicit expressions for the matrix elements of a general one-particle operator:

$$\hat{D}=\sum\ d_{rs}c_r^\dagger c_s \tag{A1}$$

with respect to the second-order ISR. Some remarks on the derivation procedure are given at the end of this section.

The general form of the ISR matrix elements of $\hat{D}$ is

$$\tilde{D}_{IJ}=\langle\tilde{\Psi}_I|\hat{D}|\tilde{\Psi}_J\rangle=\delta_{IJ}D_0+D_{IJ}, \tag{A2}$$

where $D_0=\langle\Psi_0|\hat{D}|\Psi_0\rangle$ in the diagonal term is the ground state expectation value of $\hat{D}$ [see Eqs. (31) and (32)] and $D_{IJ}$ denote the ISR matrix elements of the shifted operator $\hat{D}-D_0$. At the second- and third-order level the explicit ISR configuration space comprises the $p-h$ and $2p-2h$ states. The matrix elements in the $p-h$ diagonal block, the $p-h/2p-2h$ block, and the $2p-2h$ diagonal block are needed through second, first, and zeroth order, respectively. For notational convenience the abbreviation

$$v_{pqrs}=\frac{V_{pq[rs]}}{\epsilon_p+\epsilon_q-\epsilon_r-\epsilon_s} \tag{A3}$$

is used in the following, where $V_{pq[rs]}=V_{pqrs}-V_{pqsr}$ denotes the antisymmetrized Coulomb integrals (in ''1212'' form) and $\epsilon_p$ are HF orbital energies. As before, the subscripts $a,b,c,\ldots$ and $i,j,k,\ldots$ refer to unoccupied (virtual) and occupied orbitals, respectively, while the letters $p,q,r,\ldots$ will be used in the general case.

(a) *$p-h$ diagonal block*,

$$D_{ak,a'k'}=\delta_{kk'}d_{aa'}-\delta_{aa'}d_{k'k}+\sum_{i=1}^{7}d_{ak,a'k'}^{(2,i)}, \tag{A4}$$

where the seven second-order contributions $D_{ak,a'k'}^{(2,i)}$ are given by

$$D_{ak,a'k'}^{(2,1)}=-\delta_{kk'}\sum_l\ \rho_{la'}^{(2)}d_{al}-\delta_{aa'}\sum_b\ \rho_{k'b}^{(2)}d_{bk}+\text{h.c.}, \tag{A5}$$

$$D_{ak,a'k'}^{(2,2)}=-\frac{1}{4}\delta_{kk'}\sum_{c,d,i,j}\ v_{cdij}^*v_{adij}d_{ca'}+\text{h.c.}, \tag{A6}$$

$$D_{ak,a'k'}^{(2,3)}=-\frac{1}{2}\delta_{kk'}\sum_{c,d,i,j}\ v_{a'cij}^*v_{adij}d_{cd}+\delta_{kk'}\sum_{d,i,j,l}\ v_{a'dij}^*v_{adlj}d_{li}, \tag{A7}$$

$$D_{ak,a'k'}^{(2,4)}=\frac{1}{4}\delta_{aa'}\sum_{c,d,i,j}\ v_{cdij}^*v_{cdkj}d_{k'i}+\text{h.c.}, \tag{A8}$$

$$D_{ak,a'k'}^{(2,5)}=-\delta_{aa'}\sum_{c,c',d,j}\ v_{cdk'j}^*v_{c'dkj}d_{cc'}+\frac{1}{2}\delta_{aa'}\sum_{c,d,i,j}\ v_{cdk'j}^*v_{cdki}d_{ij}, \tag{A9}$$

$$D_{ak,a'k'}^{(2,6)}=\frac{1}{2}\sum_{c,d,j}\ v_{cdk'j}^*v_{adkj}d_{ca'}-\frac{1}{2}\sum_{d,i,j}\ v_{a'dij}^*v_{adkj}d_{k'i}+\text{h.c.}, \tag{A10}$$

$$D_{ak,a'k'}^{(2,7)}=-\sum_{d,i,j}\ v_{a'dk'j}^*v_{adki}d_{ij}+\sum_{c,d,j}\ v_{a'ck'j}^*v_{adkj}d_{cd}. \tag{A11}$$

In Eq. (A5), $\rho_{ka}^{(2)}$ denotes second-order contributions to the one-particle density matrix elements [Eq. (32)]. It is advisable to evaluate these contributions using the DEM/ADC(3) approximation as discussed in Sec. III rather than the strict second-order expression. Note that there is no first-order contribution to the diagonal $p-h$ block.

(b) *$p-h/2p-2h$ coupling block*,

$$\begin{aligned}D_{ak,a'b'k'l'}=&-\delta_{aa'}\delta_{kk'}\Big(d_{l'b'}-\sum_{d,j}\ v_{b'dl'j}^*d_{dj}\Big)\\&+\delta_{aa'}\delta_{kl'}\Big(d_{k'b'}-\sum_{d,j}\ v_{b'dk'j}^*d_{dj}\Big)\\&+\delta_{ab'}\delta_{kk'}\Big(d_{l'a'}-\sum_{d,j}\ v_{a'dl'j}^*d_{dj}\Big)\\&-\delta_{ab'}\delta_{kl'}\Big(d_{k'a'}-\sum_{d,j}\ v_{a'dk'j}^*d_{dj}\Big)\\&-\delta_{aa'}\sum_c\ v_{cb'k'l'}^*d_{ck}+\delta_{ab'}\sum_c\ v_{ca'k'l'}^*d_{ck}\\&-\delta_{kk'}\sum_j\ v_{a'b'jl'}^*d_{aj}+\delta_{kl'}\sum_j\ v_{a'b'jk'}^*d_{aj}.\end{aligned} \tag{A12}$$

(c) $2p-2h$ *diagonal block*,

$$D_{abkl,a'b'k'l'}=\delta_{bb'}\delta_{kk'}\delta_{ll'}d_{aa'}-\delta_{ba'}\delta_{kk'}\delta_{ll'}d_{ab'}+\delta_{aa'}\delta_{kk'}\delta_{ll'}d_{bb'}-\delta_{ab'}\delta_{kk'}\delta_{ll'}d_{ba'}-\delta_{aa'}\delta_{bb'}\delta_{ll'}d_{k'k}+\delta_{aa'}\delta_{bb'}\delta_{lk'}d_{l'k}-\delta_{aa'}\delta_{bb'}\delta_{kk'}d_{l'l}+\delta_{aa'}\delta_{bb'}\delta_{kl'}d_{k'l}. \tag{A13}$$

The PT expressions given here can be derived in a straightforward, though somewhat tedious way using Rayleigh–Schrödinger PT for the ground state $|\Psi_0\rangle$ in the general ISR terms. A few remarks on the procedure may be appropriate.

Let us consider the $p-h$ diagonal block, $\tilde{\mathbf{D}}_{11}$, of the ISR matrix, reading in matrix notation

$$\tilde{\mathbf{D}}_{11}=\mathbf{S}^{-1/2}\mathbf{D}_{11}^{\#}\mathbf{S}^{-1/2}. \tag{A14}$$

Here $\mathbf{S}$ is the overlap matrix [Eq. (6)],

$$S_{ak,bl}=\langle\Psi_0|c_k^\dagger c_a c_b^\dagger c_l|\Psi_0\rangle-\rho_{ak}\rho_{lb} \tag{A15}$$

of the precursor states [Eq. (4)],

$$|\Psi_{ak}^{\#}\rangle=(c_a^\dagger c_k-\rho_{ka})|\Psi_0\rangle \tag{A16}$$

and $\mathbf{D}_{11}^{\#}$ is the precursor state representation of $\hat{D}$,

$$D_{ak,bl}^{\#}=\langle\Psi_0|c_k^\dagger c_a\hat{D}c_b^\dagger c_l|\Psi_0\rangle-\rho_{lb}\langle\Psi_0|c_k^\dagger c_a\hat{D}|\Psi_0\rangle-\rho_{ak}\langle\Psi_0|\hat{D}c_b^\dagger c_l|\Psi_0\rangle+\rho_{ak}\rho_{lb}\langle\Psi_0|\hat{D}|\Psi_0\rangle. \tag{A17}$$

Let us note that the $p-h$ components,

$$\rho_{ka}=\langle\Psi_0|c_a^\dagger c_k|\Psi_0\rangle\sim O(2) \tag{A18}$$

of the one-particle density matrix are of second order of PT, so that the last term on the rhs of Eq. (A17) does not come into play before fourth order. As can readily be seen, the perturbation expansion of $\mathbf{S}$ is of the form

$$\mathbf{S}=\mathbf{1}+\mathbf{S}^{(2)}+O(3). \tag{A19}$$

Using

$$\mathbf{S}^{-1/2}=\mathbf{1}-\tfrac{1}{2}\mathbf{S}^{(2)}+O(3) \tag{A20}$$

we find

$$\tilde{\mathbf{D}}_{11}=\mathbf{D}_{11}^{\#(0)}+\mathbf{D}_{11}^{\#(1)}+\mathbf{D}_{11}^{\#(2)}-\tfrac{1}{2}(\mathbf{S}^{(2)}\mathbf{D}_{11}^{\#(0)}+\mathbf{D}_{11}^{\#(0)}\mathbf{S}^{(2)})+O(3) \tag{A21}$$

for the expansion of $\mathbf{D}_{11}$ through second order. Here the zeroth-order contribution is simply given by

$$D_{ak,bl}^{\#(0)}=\langle\Phi_0|c_k^\dagger c_a\hat{D}c_b^\dagger c_l|\Phi_0\rangle, \tag{A22}$$

where $|\Phi_0\rangle$ denotes the HF ground state. As can readily be seen, the first-order contribution vanishes: $D_{ak,bl}^{\#(1)}=0$. In the second-order part,

$$D_{ak,bl}^{\#(2)}=\langle\Psi_0^{(2)}|c_k^\dagger c_a\hat{D}c_b^\dagger c_l|\Phi_0\rangle+\text{h.c.}+\langle\Psi_0^{(1)}|c_k^\dagger c_a\hat{D}c_b^\dagger c_l|\Psi_0^1\rangle-\rho_{lb}^{(2)}d_{ak}-\rho_{ak}^{(2)}d_{bl}-\tfrac{1}{2}(\mathbf{S}^{(2)}\mathbf{D}_{11}^{\#(0)}+\mathbf{D}_{11}^{\#(0)}\mathbf{S}^{(2)})_{ak,bl} \tag{A23}$$

one has to deal with four different contributions (i)–(iv): The first (i) and second (ii) contribution arise from the PT expansion of the first term on the right-hand side of Eq. (A23); contribution (iii) comprises the two $\rho^{(2)}d$ terms arising from the orthogonalization of the intermediate states with respect to $|\Psi_0\rangle$, while the two $\mathbf{S}^{(2)}\mathbf{D}^{\#(0)}$ terms associated with the IS normalization are collected in contribution (iv). For treating (i) and (ii) it is helpful to use the commutator relation

$$[c_k^\dagger c_a,\hat{D}]=\sum_s d_{as}c_k^\dagger c_s-\sum_r d_{rk}c_r^\dagger c_a \tag{A24}$$

and replace $c_k^\dagger c_a\hat{D}$ in (i) and (ii) according to

$$c_k^\dagger c_a\hat{D}=\hat{D}c_k^\dagger c_a+\sum_s d_{as}c_k^\dagger c_s-\sum_r d_{rk}c_r^\dagger c_a. \tag{A25}$$

Thereby one avoids having to evaluate matrix elements of $\hat{D}$ with respect to triple excitations on the HF ground state. Moreover, several distinct contributions split off in a quite natural way:

- $\delta_{ab}\delta_{kl}\langle\Psi_0|\hat{D}|\Psi_0\rangle^{(2)}$ [from (i) and (ii)],
- part of (i) cancels exactly (iii),
- $(\delta_{kl}d_{ab}-\delta_{ab}d_{lk})\langle\Psi_0|\Psi_0\rangle^{(2)}=0$ [from (i) and (ii)],
- the contribution (iv) is canceled completely by terms arising from (ii).

The evaluation of (i) is simple; note that only the $p-h$ part of $|\Psi_0^{(2)}\rangle$ comes into play. The result (after cancellations) is given by Eq. (A5). The (ii) part is more intricate. The partitioning according to Eq. (A25) leads to three distinct parts, (A)–(C). Here part (A) contributes to all six Eqs. (A6)–(A11), (B) to (A6) and (A10), and (C) to (A8) and (A10). Note that in (A) one has to deal with matrix elements of the type $\langle 2p-2h|\hat{D}|2p-2h\rangle$.

For the $p-h/2p-2h$ matrix elements, $\langle\tilde{\Psi}_{ak}|\hat{D}|\tilde{\Psi}_{abkl}\rangle$, the intermediate states are needed through first order only,

$$|\tilde{\Psi}_{ak}\rangle=c_a^\dagger c_k|\Phi_0\rangle+c_a^\dagger c_k|\Psi_0^{(1)}\rangle+O(2), \tag{A26}$$

$$|\tilde{\Psi}_{abkl}\rangle=c_a^\dagger c_b^\dagger c_k c_l|\Phi_0\rangle-|\Phi_0\rangle\langle\Psi_0^{(1)}|c_a^\dagger c_b^\dagger c_k c_l|\Phi_0\rangle+O(2). \tag{A27}$$

The ensuing evaluation of the matrix elements (through first order) is straightforward.

[1] T. Helgaker, P. Jørgensen, and J. Olsen, *Molecular Electronic Structure Theory* (Wiley, New York, 2000).
[2] K. Andersson, P.-Å. Malmquist, B. O. Roos, A. Sadlej, and K. Wolinski, J. Phys. Chem. **94**, 5483 (1990).
[3] K. Andersson, P.-Å. Malmquist, and B. O. Roos, J. Chem. Phys. **96**, 1218 (1992).
[4] E. Dalgaard and H. J. Monkhorst, Phys. Rev. A **28**, 1217 (1983).
[5] H. Koch and P. Jørgensen, J. Chem. Phys. **93**, 3333 (1990).

[6] H. Koch, H. J. A. Jensen, P. Jørgensen, and T. Helgaker, J. Chem. Phys. **93**, 3345 (1990).
[7] H. Sekino and R. J. Bartlett, Int. J. Quantum Chem., Quantum Chem. Symp. **18**, 255 (1984).
[8] J. Geertsen, M. Rittby, and R. J. Bartlett, Chem. Phys. Lett. **164**, 57 (1989).
[9] J. F. Stanton and R. J. Bartlett, J. Chem. Phys. **98**, 7029 (1993).
[10] H. Nakatsuji and K. Hirao, Chem. Phys. Lett. **47**, 569 (1977).
[11] H. Nakatsuji, Chem. Phys. Lett. **67**, 329 (1979).
[12] H. Nakatsuji, Chem. Phys. Lett. **67**, 334 (1979).
[13] H. Koch, R. Kobayashi, A. S. De Meras, and P. Jørgensen, J. Chem. Phys. **100**, 4393 (1994).
[14] O. Christiansen, A. Halkier, H. Koch, P. Jørgensen, and T. Helgaker, J. Chem. Phys. **108**, 2801 (1998).
[15] O. Christiansen, P. Jørgensen, and C. Hättig, Int. J. Quantum Chem. **68**, 1 (1998).
[16] E. K. U. Gross and W. Kohn, Adv. Quantum Chem. **21**, 255 (1990).
[17] M. E. Casida, in *Recent Advances in Density Functional Theory, Part I*, edited by D. P. Chong (World Scientific, Singapore, 1994).
[18] C. Van Caillie and R. D. Amos, Chem. Phys. Lett. **308**, 249 (1999).
[19] C. Van Caillie and R. Amos, Chem. Phys. Lett. **317**, 159 (2000).
[20] R. Burcl, R. D. Amos, and N. Handy, Chem. Phys. Lett. **355**, 8 (2002).
[21] A. L. Fetter and J. D. Walecka, *Quantum Theory of Many-Particle Systems* (McGraw-Hill, New York, 1971).
[22] J. Oddershede, Adv. Quantum Chem. **11**, 275 (1978).
[23] J. Oddershede, Adv. Chem. Phys. **69**, 201 (1987).
[24] K. L. Bak, H. Koch, J. Oddershede, O. Christiansen, and S. P. A. Sauer, J. Chem. Phys. **112**, 4173 (2000).
[25] J. Schirmer, Phys. Rev. A **26**, 2395 (1982).
[26] A. B. Trofimov and J. Schirmer, J. Phys. B **28**, 2299 (1995).
[27] A. B. Trofimov, G. Stelter, and J. Schirmer, J. Chem. Phys. **111**, 9982 (1999).
[28] A. B. Trofimov, G. Stelter, and J. Schirmer, J. Chem. Phys. **117**, 6402 (2002).
[29] D. Goscinski and B. Lukman, Chem. Phys. Lett. **7**, 573 (1970).
[30] D. J. Rowe, Rev. Mod. Phys. **40**, 153 (1968).
[31] J. Rose, T. Shibuya, and V. McKoy, J. Chem. Phys. **58**, 74 (1973).
[32] B. Weiner and Y. Öhrn, J. Phys. Chem. **91**, 563 (1987).
[33] J. Schirmer, Phys. Rev. A **43**, 4647 (1991).
[34] F. Mertins and J. Schirmer, Phys. Rev. A **53**, 2140 (1996).
[35] J. Schirmer, A. B. Trofimov, and G. Stelter, J. Chem. Phys. **109**, 4734 (1998).
[36] J. Schirmer and G. Angonoa, J. Chem. Phys. **91**, 1754 (1989).
[37] J. Schirmer and A. Thiel, J. Chem. Phys. **115**, 10621 (2001).
[38] J. Schirmer and F. Mertins, Int. J. Quantum Chem. **58**, 329 (1996).
[39] M. W. Schmidt, K. K. Baldridge, J. A. Boatz, *et al.*, J. Comput. Chem. **14**, 1347 (1993).
[40] J. S. Binkley, J. A. Pople, and W. Hehre, J. Am. Chem. Soc. **102**, 939 (1980).
[41] J. Ivanic and K. Ruedenberg, Determinantal full CI program, AMES Laboratory, 1998.
[42] J. A. Barltrop and J. D. Coyle, *Excited States in Organic Chemistry* (Wiley, London, 1975).
[43] W. Liptay, in *Excited States*, edited by C. Lim (Academic, New York, 1974), Vol. 1.
[44] S. P. Karna, P. N. Prasad, and M. Dupuis, J. Chem. Phys. **94**, 1171 (1991).
[45] H. Ågren, O. Vahtras, H. Koch, P. Jørgensen, and T. Helgaker, J. Chem. Phys. **98**, 6417 (1993).
[46] K. V. Mikkelsen, Y. Luo, H. Ågren, and P. Jørgensen, J. Chem. Phys. **100**, 8240 (1994).
[47] D. Jonsson, P. Norman, H. Ågren, Y. Luo, K. O. Sylvester-Hvid, and K. Mikkelsen, J. Chem. Phys. **109**, 6351 (1998).
[48] R. Wortmann, P. Krämer, C. Glania, S. Lebus, and N. Detzer, Chem. Phys. **173**, 99 (1993).
[49] W. Schuddeboom, J. M. Warman, H. A. Biemans, and E. W. Meijer, J. Phys. Chem. **100**, 12369 (1996).
[50] V. M. Farztdinov, R. Schanz, S. A. Kovalenko, and N. P. Ernsting, J. Phys. Chem. A **104**, 11486 (2000).
[51] P. Salek, O. Vatras, T. Helgaker, and H. Ågren, J. Chem. Phys. **117**, 9630 (2002).
[52] A. M. Moran and A. M. Kelley, J. Chem. Phys. **115**, 912 (2001).
[53] A. M. Moran, A. M. Kelley, and S. Tretiak, Chem. Phys. Lett. **367**, 293 (2003).
[54] A. Becke, J. Chem. Phys. **98**, 5648 (1993).
[55] C. Lee, W. Yang, and R. Parr, Phys. Rev. B **37**, 785 (1988).
[56] T. H. Dunning, J. Chem. Phys. **90**, 1007 (1989).
[57] M. J. Frisch, G. W. Trucks, H. B. Schlegel, *et al.*, GAUSSIAN 98, Revision A.7, Gaussian, Inc., Pittsburgh, PA, 1998.
[58] W. J. Hehre, R. Ditchfield, and J. A. Pople, J. Chem. Phys. **56**, 2257 (1972).
[59] L. Serrano-Andrés, M. P. Fülscher, and G. Karlström, Int. J. Quantum Chem. **65**, 167 (1997).
[60] T. Clark, J. Chandrasekhar, and P. v. R. Schleyer, J. Comput. Chem. **4**, 294 (1983).
[61] L. Serrano-Andrés, M. Merchan, I. Nebot-Gil, B. Roos, and M. Fülscher, J. Am. Chem. Soc. **115**, 6184 (1993).
[62] A. B. Trofimov and J. Schirmer, Chem. Phys. **214**, 153 (1997).
[63] O. Christiansen, J. Gauss, J. F. Stanton, and P. Jørgensen, J. Chem. Phys. **111**, 525 (1999).
[64] B. O. Roos, P.-Å. Malmqvist, V. Molina, L. Serrano-Andrés, and M. Merchan, J. Chem. Phys. **116**, 7526 (2000).
[65] M. J. S. Dewar, C. Jie, and J. Yu, Tetrahedron **49**, 5003 (1993).
[66] A. B. Trofimov, J. Schirmer, and J. Breidbach (unpublished).